A Completely Theoretical Design Method of Dielectric Image Guide Gratings in the Bragg Reflection Region

HIROSHI SHIGESAWA, SENIOR MEMBER, IEEE, AND MIKIO TSUJI, MEMBER, IEEE

Abstract —**This paper presents a new and completely theoretical accurate method for the design of dielectric image guide gratings. Our method is based on a network approach that can easily analyze, with satisfactory approximations, the interaction of dielectric step discontinuities. These are the fundamental constituents of our gratings. Measurements on a filter modeled at X-band show excellent agreement with the design characteristics.**

I. Introduction

SIGNIFICANT PROGRESS has been made recently in millimeter wave technology, much of that is largely on extension of microwave techniques. As for the waveguide structures for integrated circuit use, printed-line type waveguides such as microstrip line and finline have produced much success in circuitries and subsystems.

For the shorter millimeter wavelengths, however, the smaller structure sizes and higher metal losses make those structures no longer practical, and new structures and techniques must be investigated. One of alternatives to printed-line type millimeter-wave integrated circuits will be dielectric waveguide structures [1]–[3]. However, relatively little has been investigated on procedures for designing practical circuitries utilizing such a waveguide.

One of exceptions is in the work of Matthaei *et al.* [4], which presented a method for the design of dielectric image guide (DIG) gratings. Matthaei and his coworkers also applied their method to obtain some DIG filters [5]. We investigate here the DIG gratings that are similar to theirs. Their method is based on a combination of approximate theory and measurements on trial gratings. Although it seems simple, the requirement of experimental data in the numerical design stage is a serious disadvantage.

On the contrary, our method presented here is a completely theoretical one that needs no experimental data and is based on the analysis of dielectric step discontinuities and their cascaded connection. The general idea of our method has been extensively discussed in relation to the step discontinuity problem in open dielectric waveguides and its application to any kinds of periodic structure with finite length [6]–[9]. The discontinuity problems of isolated steps have been discussed in [6] by accurately taking account of both surface-wave modes and the waves with continuous spectrum. An effective microwave network representation has been derived for a step discontinuity including radiation phenomena in [7]. Afterwards, such a network approach has been successfully applied to periodic structures with finite length, operating not only in their stop bands [8], but also in a different regime of operation corresponding to the leaky wave region [9].

The works mentioned above have clearly shown that in so far as the first Bragg reflection region is used, the energy carried away by the continuous waves is negligible and we may consider only surface-wave ports in the equivalent network representation. This validity has been successfully demonstrated in our previous paper [10] in the case of gratings on an H-guide. The method presented here has a great theoretical advance in enabling the design of gratings on three-dimensional (3-D) dielectric waveguides of an open type.

Manuscript received August 6, 1985; revised November 14, 1985. This work was supported in part by the Science and Engineering Research Institute of Doshisha University under a Grant-in-Aid.

The authors are with the Department of Electronics, Doshisha University, Kamikyo-ku, Kyoto, 602 Japan.

II. Propagation Constant and Junction Discontinuity of DIG

The DIG structure investigated here is depicted in Fig. 1, which is similar with Fig. 2(a) of [4]. The periodic rectangular corrugations or notches are put on the sides of the guide within the limits of a finite length along the guide axis (the z-axis).

Although a uniform DIG along the z-axis supports hybrid modes with all six field components, we may often classify the modes into two approximate groups: one is the E_{mn}^{y} mode group, for which the E field is predominantly vertically polarized in the y-direction, while the other is the E_{mn}^{x} mode group, for which the E field is predominantly horizontally polarized in the x-direction. As discussed in [11], the use of corrugations as in Fig. 1 is decidedly superior to the corrugations put on top of DIG insofar as the lowest order E_{11}^{y} mode is concerned. As seen from Fig. 1, this structure can be viewed as consisting of many dielectric step discontinuities connected by a length of uniform DIG. For realizing a completely theoretical design of DIG gratings, it is necessary to derive an equivalent network characterizing a step discontinuity between two DIG's with different cross-sectional dimensions, and also

0018-9480/86/0400-0420$01.00

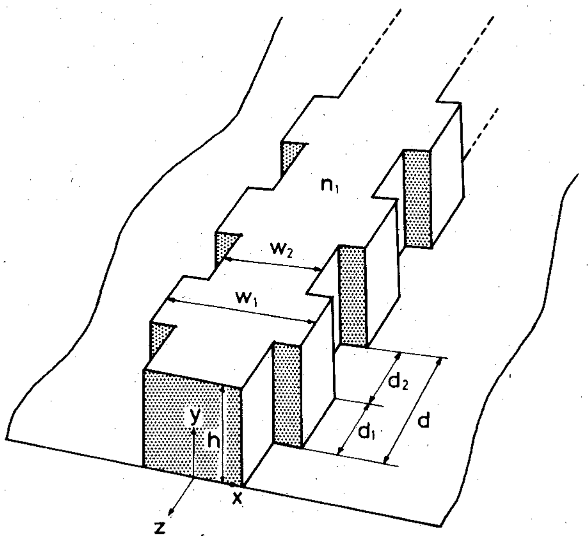

Fig. 1. Dielectric image guide gratings consisting of a finite length of periodic corrugations or notches.

to calculate accurately the propagation constant in each DIG. In the following two subsections, these problems will be discussed separately.

A. Propagation Constant and Field Distribution of Dielectric Image Guides

Fig. 2 shows the cross section of the ith DIG (i = I or II, dielectric dimension is $w_i \times h$ and its refractive index is n_1). We assume the refractive index of the outside air region to be $n_2 = 1$ and indicate the boundary contour of DIG by Γ_i.

We first expand the electromagnetic fields of the E_{11}^y mode into a series of circular harmonics, as Goell did [12], as follows.

Dielectric Region:

$$e_{z1}^i = \sum_m A_m^i J_m(\rho_i r) \sin(m\theta) \tag{1}$$

$$h_{z1}^i = \sum_m B_m^i J_m(\rho_i r) \cos(m\theta) \tag{2}$$

Air Region:

$$e_{z2}^i = \sum_m C_m^i K_m(\kappa_i r) \sin(m\theta) \tag{3}$$

$$h_{z2}^i = \sum_m D_m^i K_m(\kappa_i r) \cos(m\theta) \tag{4}$$

where the exponential dependence exp $j(\omega t - \beta_i z)$ is abbreviated and the transverse propagation constants are given by

$$\rho_i^2 = (n_1 k_0)^2 - \beta_i^2$$
$$\kappa_i^2 = \beta_i^2 - k_0^2 \tag{5}$$

where $k_0^2 = \omega^2 \mu_0 \epsilon_0$. The J_m and K_m are the mth order Bessel functions and modified Bessel functions, respectively. The r and θ components of the field can then be obtained by substituting (1) and (2) or (3) and (4) into Maxwell's equations. It should be noted that the integer m is always odd $(2n-1)$, $(n = 1, 2, \cdots)$ because of the symmetry of the E_y component of the E_{11}^y mode with respect to the $y-z$ plane at $x = 0$.

The propagation constant is obtained by considering the boundary condition on the boundary contour Γ_i, that is, $\boldsymbol{n} \times (\boldsymbol{e}_1^i - \boldsymbol{e}_2^i) = 0$ and $\boldsymbol{n} \times (\boldsymbol{h}_1^i - \boldsymbol{h}_2^i) = 0$ ($\boldsymbol{n}$ is the unit vector normal to both Γ_i and the z axis: $\mathfrak{e}$ and $\mathfrak{h}$ are the total electric and magnetic fields). However, the infinite series in (1)–(4) should be truncated to a finite number of terms M in practical calculations. Such approximated fields never satisfy the above type of boundary conditions. We therefore fit the approximated fields to this boundary condition in the sense of least-squares [13], instead of the point matching method [12]. For this purpose, we define the mean-square error $g_{\Gamma i}$ in the boundary condition by the following equation:

$$g_{\Gamma i} = \int_{\Gamma_i} \left\{ \left| \boldsymbol{n} \times \left(\boldsymbol{e}_1^i - \boldsymbol{e}_2^i \right) \right|^2 + Z^2 \left| \boldsymbol{n} \times \left(\boldsymbol{h}_1^i - \boldsymbol{h}_2^i \right) \right|^2 \right\} ds$$
$$+ \xi \left(A_1^{i*} - 1 \right) + \xi^* \left(A_1^i - 1 \right) \tag{6}$$

where Z, an arbitrary impedance parameter, is not uniquely defined, and the intrinsic impedance of the dielectric region, $Z_1 = \sqrt{\mu_0 / n_1^2 \epsilon_0}$, is used as Z in the following calculations. ξ means a Lagrange multiplier and * indicates the complex conjugate. As mentioned before, there is a symmetry in the E_{11}^y mode field, and we have only to do the integration of (6) along Γ_i in the first quadrant. After performing the integration of (6), we obtain the error g_{Γ_i} as a function of both the modal coefficients and ξ, which are solved by applying the Ritz–Galerkin variational approach to g_{Γ_i}. This results in the relation $g_{\Gamma_i} = -\xi$, and the propagation constant β_i can be obtained by minimizing this ξ [14].

Table I shows an example of calculated β_i for DIG's of polyethylene ($n_1 = 1.52$) with different w_i / λ_0 values ($\lambda_0 =$

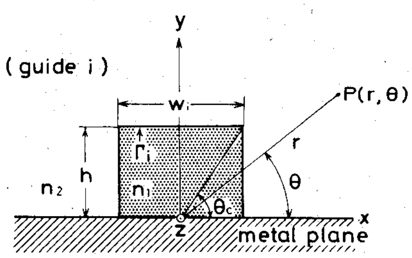

Fig. 2. Cross-sectional view of DIG and the coordinate system.

TABLE I
CONVERGENCE PROPERTY OF PROPAGATION CONSTANT

N	β_1/k_0	β_2/k_0
2	1.319	1.253
3	1.314	1.251
4	1.316	1.252
5	1.316	1.252
6	1.316	1.252
7	1.317	1.252
8	1.317	1.252

Note: ($n_1 = 1.52$, guide I: $w_1/\lambda_0 = 0.633$, $h/\lambda_0 = 0.4$, guide II: $w_2/\lambda_0 = 0.433$, and $h/\lambda_0 = 0.4$).

free space wavelength). $N\ (=(M+1)/2)$ means the number of expansion terms in (1)–(4). It is clear that the propagation constants for both DIG's almost converge for $N \geqq 7$. Thus $N=9$ is used in the following calculations, unless a DIG has extremely large or small w_i/h value.

B. Junction of Two DIG's with Different Cross-Sectional Dimensions

The junction discontinuity that we are concerned with here is depicted in Fig. 3. The guide I has the width w_1 and the guide II has the width w_2 ($< w_1$); both guides have the same height h and are connected at $z=0$, symmetrically in the $x-y$ plane. It is assumed that both DIG's support only the E_{11}^y mode and produce negligible radiation losses at their junction. Thus, only the fields of the lowest-order mode are assumed in each section of guide, and the junction reflection and transmission coefficients are adjusted to optimize the match of the field at the step junction.

For the mode incidence from the guide I, let the amplitude reflection and transmission coefficients be R_{11} and T_{21}, which make it possible to write the tangential components to the $x-y$ plane at $z=0$ as follows:

$$E_{\eta j}^{\mathrm{I}} = (1+R_{11})e_{\eta j}^{\mathrm{I}}, \quad H_{\eta j}^{\mathrm{I}} = (1-R_{11})h_{\eta j}^{\mathrm{I}}$$

$$E_{\eta j}^{\mathrm{II}} = T_{21}e_{\eta j}^{\mathrm{II}}, \qquad H_{\eta j}^{\mathrm{II}} = T_{21}h_{\eta j}^{\mathrm{II}},$$

$$(\eta = r \text{ or } \theta, \ j=1 \text{ or } 2). \tag{7}$$

In (7), the following normalization in each guide ($i=$ I or II) should be considered:

$$\sum_{j=1}^{2} \int_{s_j} \left(e_{rj}^i h_{\theta j}^i - e_{\theta j}^i h_{rj}^i\right) ds = 1 \tag{8}$$

where the integration area S_1 covers the cross-sectional area of a guide, while the area S_2 covers the outside of it.

For solving R_{11} and T_{21} through the continuity condition of fields at the junction plane of two DIG's, we again define the mean-square error g_s in the continuity condition by the following equation:

$$g_s = \frac{\int_s \left|z_0 \times \left(E_\nu^{\mathrm{I}} - E_\mu^{\mathrm{II}}\right)\right|^2 ds}{\sum_{j=1}^{2} \int_{s_j} \left|z_0 \times e_j^{\mathrm{I}}\right|^2 ds} + \frac{\int_s \left|z_0 \times \left(H_\nu^{\mathrm{I}} - H_\mu^{\mathrm{II}}\right)\right|^2 ds}{\sum_{j=1}^{2} \int_{s_j} \left|z_0 \times h_j^{\mathrm{I}}\right|^2 ds} \tag{9}$$

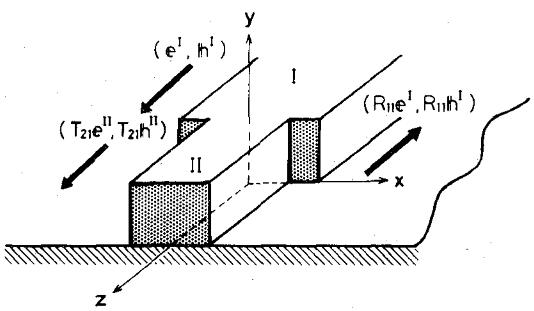

Fig. 3. Stepwise junction discontinuity of two differently sized DIG's.

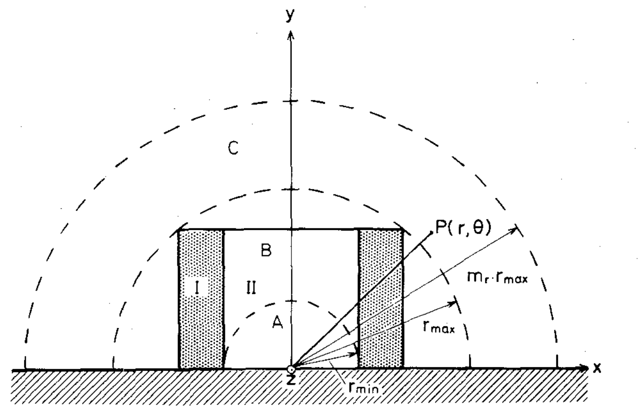

Fig. 4. Junction discontinuity plane and the division of its area for approximating the integrations in (9).

TABLE II
CONVERGENCE PROPERTY OF THE SCATTERING MATRIX ON THE INTEGRATION AREA

m_r	S_{11}	S_{22}
2	0.046070	-0.044875
5	0.046141	-0.045039
10	0.046141	-0.045039

Note: ($n_1 = 1.52$, $w_1/\lambda_0 = 0.633$, $w_2/\lambda_0 = 0.433$, and $h/\lambda_0 = 0.4$).

where $\mathbf{z}_0$ means the unit vector to the z direction. As will be discussed below, the integration area S of the numerator is approximated by a limited one in the $x-y$ plane in practical calculations. Then we have to choose ν and μ correspondingly properly to $j=1$ or 2. Thus, R_{11} and T_{21} can be solved by minimizing the error g_s with respect to these unknows.

Following the same method, R_{22} and T_{12} can be obtained by considering the E_{11}^y mode incidence from the guide II. These R_{pp} and T_{pq} (p, $q=1$, 2) result in the scattering matrix with 2×2 elements characterizing the junction discontinuity, which is often transformed into the transmission matrix for ease of calculations in cascaded connection of discontinuities.

Now, the problem remaining is to approximate the integration area S of the numerator in (9). We divide the whole junction plane into four regions, as shown in Fig. 4: region A is the area inside the inscribed circle with the radius $r_{\min}$ to the guide II; region B is the area lying between $r_{\min}$ and the circumcircle with the radius $r_{\max}$ to the guide I; region C is the area lying between $r_{\max}$ and an arbitrary radius $m_r \cdot r_{\max}$ (m_r a constant larger than unity); and the rest outside $m_r \cdot r_{\max}$ is disregarded here by taking into account the convergence of solutions with respect to m_r. According to this division of S, we may perform the integrations analytically with respect to θ and numerically with respect to r in both regions A and C, while the integrations are numerically performed with respect to both r and θ in region B. This approach is superior, from the viewpoint of numerical accuracy, to the full numerical integrations inside the circle of the radius $m_r \cdot r_{\max}$. Table II shows an example of the convergence check for the ele-

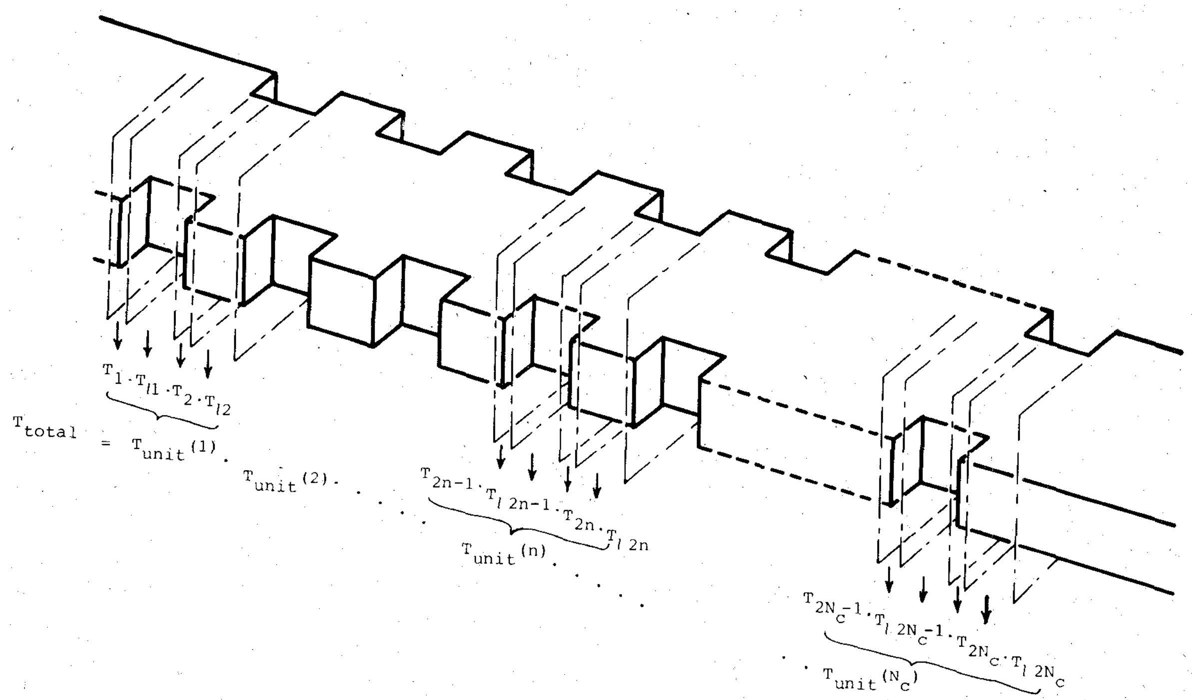

Fig. 5. DIG gratings consisting of a finite length of corrugations. $T_{\mathrm{unit}}\,(n)$ means the transmission matrix of the nth unit cell.

ments S_{11} and S_{22} of a scattering matrix as a multiplier m_r is varied. It is clear that the solutions barely converge at $m_r = 5$, and, hereafter, $m_r = 10$ is considered for satisfactory calculations.

III. Analytical and Experimental Discussions on DIG Gratings with a Finite Length

As shown in Fig. 1, a DIG grating with a finite length can be viewed as consisting of a finite number of step junctions connected by lengths of uniform DIG. The propagation characteristics are then analyzed by a cascaded connection of the transmission matrices of both the junction discontinuity ($\boldsymbol{T}_n$ for the nth junction) and the uniform DIG ($\boldsymbol{T}_{ln}$ for the nth DIG). Such an approximate approach is valid as far as the first Bragg reflection region is concerned as mentioned before. Using the matrices denoted above, one can define a unit cell corresponding to one period of the structure, of which the matrix can be denoted as $\boldsymbol{T}_{\mathrm{unit}}(n) = \boldsymbol{T}_{2n-1}\cdot \boldsymbol{T}_{l2n-1}\cdot \boldsymbol{T}_{2n}\cdot \boldsymbol{T}_{l2n}$, as shown in Fig. 5. Then, the transmission matrix $\boldsymbol{T}_{\mathrm{total}}$ for the finite periodic grating consisting of N_c unit cells can be given as follows:

$$\boldsymbol{T}_{\mathrm{total}} = \prod_{n=1}^{N_c} \boldsymbol{T}_{\mathrm{unit}}(n). \tag{10}$$

This $\boldsymbol{T}_{\mathrm{total}}$ easily leads to the reflection and transmission coefficients for the structure shown in Fig. 5, in case of the E_{11}^y mode incidence from one side of the structure. The above approach holds the key of development of a completely theoretical design method for DIG gratings, as shown in the next section.

Before discussing the details of our design method, it is important to confirm the validity of the approach mentioned above.

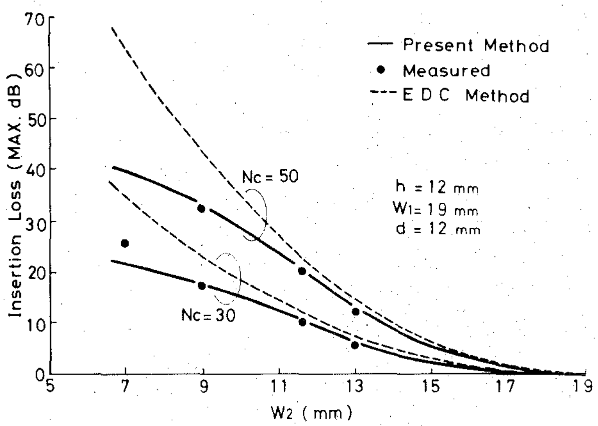

Fig. 6. Comparison between numerical and experimental results of the mid-stopband attenuation $A_{\max}$ for varying w_2.

To this end, the mid-stopband attenuation $A_{\max}$ is discussed numerically and experimentally for the DIG gratings, made of polyethylene ($n_1 = 1.52$), with $h = 12$ mm, $w_1 = 19$ mm, $d = 12$ mm, and $d_1/d_2 = 1$[1], with varying w_2[2] and N_c. Fig. 6 shows the results obtained in a 10-GHz region, where the solid curves indicate the numerical results of $A_{\max}$ calculated by the present method for $N_c = 30$ and $N_c = 50$, and the dotted curves show the results obtained by the method suggested by Matthaei *et al.* in [4] that use the approximate equations based on the effective dielectric constant (EDC) method. On the

[1] Considering the dispersion characteristic of β_t in relation to the guide width, the condition $d_1/d_2 = 1$ is slightly away from that producing the maximum attenuation. However, as will be shown later, the resultant decrease in attenuation is negligible, and $d_1/d_2 = 1$ will be a good approximation.

[2] It should be noted that the stopband center (the first Bragg) frequency is slightly changed with varying w_2 because of a constant period d.

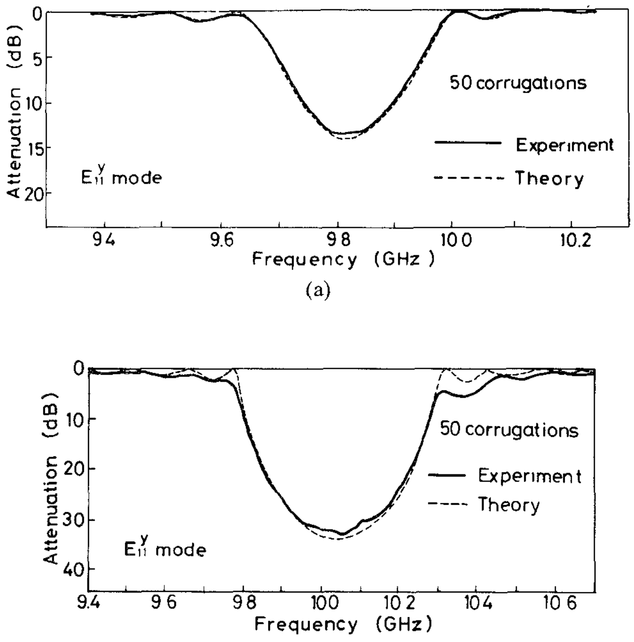

Fig. 7. (a) Frequency characteristics of the DIG gratings with shallow notch ($h = 12$mm, $w_1 = 19$mm, $w_2 = 13$mm, $d = 12$mm, and $d_1/d_2 = 1$). (b) Frequency characteristics of the DIG gratings with deep notch ($h = 12$mm, $w_1 = 19$mm, $w_2 = 9$mm, $d = 12$mm, $d_1/d_2 = 1$).

other hand, the dots indicate the measured values, and it is confirmed that our results agree surprisingly well with the measured ones even for the deep notch range with large w_2 ($w_1/w_2 = 2$ or more).

Fig. 7(a) and (b) show the frequency characteristics for the gratings ($w_1 = 19$ mm, $N_c = 50$) with the shallow notch ($w_2 = 12$ mm) and the deep notch ($w_2 = 9$ mm). These examples show good agreement between the theoretical and the experimental values. As a result of these discussions, we may proceed to the next stage: the development of a design procedure based on the present method.

IV. Design Consideration of DIG Gratings

A. Design Procedures

As seen from Fig. 1, DIG gratings have many variables to fit the characteristics to the given specifications, and this paper makes the refractive index n_1 and N_c constant and assumes $h = \alpha w_1$ (α, an arbitrary constant). Here, we denote the specified stopband center frequency and the required mid-stopband attenuation by f_0 (the corresponding free space wavelength is λ_0) and $A_{\max}$, respectively, and use the normalized dimensions like $H = h/\lambda_0$ and $W_i = w_i/\lambda_0$ ($i = 1, 2$).

We first calculate the dispersion curves as a function of W_1 with parameter α, from which the possible pairs of W_1 and H are obtained by considering that such a guide can support only the E_{11}^y mode in the required bandwidth. For each pair of (W_1, H), the procedure of Section II-B makes it possible to calculate the scattering matrix of a junction of two DIG's as a function of W_2/W_1. On the other hand, a given DIG grating shows the maximum attenuation when

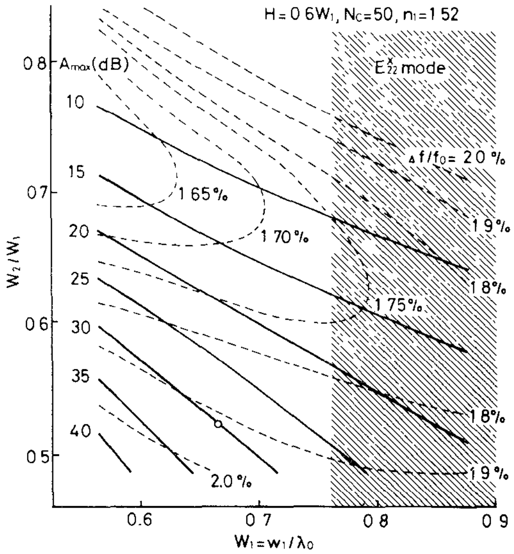

Fig. 8. Design chart of DIG gratings (the relation between W_1 and W_2 for a given specifications).

each guide length d_i (see Fig. 1) coincides with the (guide wavelength / 4) at $f = f_0$[3]. Therefore, the grating design completes when the ratio W_2/W_1 is defined in order for $A_{\max}$ to satisfy the required value. Of course, this $A_{\max}$ can be calculated by the cascaded connection of a finite number (N_c) of transmission matrices consisting of the junction matrices and uniform waveguide matrices at $f = f_0$.

One of the important parameters for expressing grating characteristics is the fractional 3-dB bandwidth $\Delta f/f_0$ (3-dB bandwidth below $A_{\max}$). This parameter, however, is fixed uniquely through the defined structural dimensions, and here the bandwidth is numerically obtained after the calculation of the insertion characteristics. Since the field distributions in the plane transverse to the z-axis varies from frequency to frequency in 3-D dielectric waveguides of the open type, following the method presented in Section II-B for all the frequencies in the stopband consumes much time in the above calculations. To reduce consuming time, we calculate here the insertion losses by using the dispersion curve obtained by the EDC method for all the frequencies in the stopband except the center frequency f_0. It has been confirmed that this approximation in obtaining the propagation constants produces no significant difference in results insofar as we take account of a compensation in which the EDC propagation constant f_0 varies with frequency proportionally to the way that our theoretical one varies in f_0 and its vicinity (Matthaei *et al.* [4] used a similar approach employing the "measured" value instead of our "theoretical" value).

Following the procedures mentioned above, a CAD program has been successfully developed. In this section, however, we show the design charts of the DIG gratings obtained from that program. An example ($H = 0.6W_1$, $n_1 = 1.52$, $N_c = 50$) is shown in Fig. 8, where the solid

[3]Since the present method considers only the surface-wave modes, we neglect here the effect of junction reactances due to the stored energy around a junction.

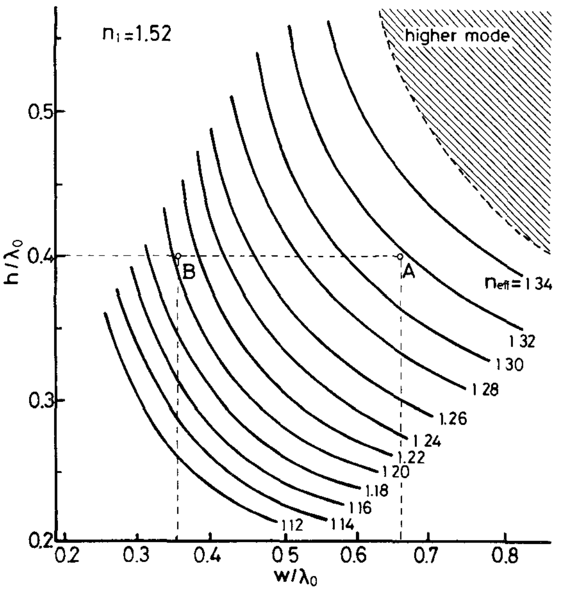

Fig. 9. Design chart of DIG gratings. This chart is used along with Fig. 8 that defines the necessary H and W for uniform guide section, from which n_{eff} is obtained (the points A and B define the necessary n_{eff}'s that realize the specifications given by the circle on Fig. 8).

curves indicate the contours of the required maximum attenuation A_{max} (dB) in the W_1–W_2/W_1 plane and the dotted curves show the corresponding $\Delta f/f_0$ in percent. In the hatched region, the next higher-order propagating mode E_{22}^x can couple with the E_{11}^y mode in the present structure, and it is desirable to set the mid-stopband frequency away from this region unless the additional stopbands due to mode coupling [15] are considered positively.

Fig. 9 shows the dependence of the equivalent refractive index $n_{eff} = \beta/k_0$ on both the guide width W and the height H. Therefore, knowing, from Fig. 8, the guide widths W_1 and W_2 that satisfy the given grating specifications, one can obtain n_{eff_i} corresponding to each W_i from Fig. 9. This n_{eff_i} finally defines the length d_i of each DIG as follows:

$$d_i = \lambda_0 \cdot (4n_{eff_i})^{-1}, \qquad i = 1, 2. \tag{11}$$

B. Design Example and Experiments

Let us consider here the following specifications:

$$f_0 = 10 \text{ GHz} \qquad (\lambda_0 = 30 \text{ mm})$$
$$A_{max} = 30 \text{ dB}$$
$$\Delta f/f_0 = 1.92 \text{ percent}$$

and design the DIG grating by using Figs. 8 and 9. These specifications can be realized by the point (W_1, W_2/W_1) indicated by the small circle on Fig. 8, i.e., $W_1 = 0.667$, $W_2/W_1 = 0.525$ and $H = 0.4$, thereby yielding $w_1 = 20$ mm, $w_2 = 10.5$ mm, and $h = 12$ mm. On the other hand, the points $A(W_1, H)$ and $B(W_2, H)$ on Fig. 9 derive $n_{eff_1} = 1.318$ and $n_{eff_2} = 1.204$, respectively, thereby resulting in $d_1 = 5.69$ mm and $d_2 = 6.23$ mm from (11). The grating design has now been finished. In the above case, the higher-order E_{22}^x mode begins to propagate in the DIG with W_1 from about 11 GHz.

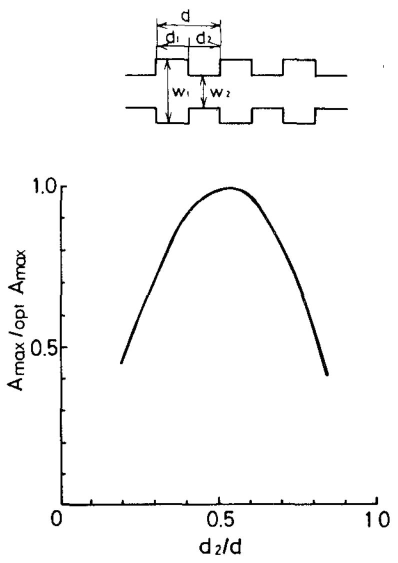

Fig. 10. Dependence of the maximum attenuation A_{max} on d_2/d (h = 12mm, w_1 = 20mm, and w_2 = 10.5mm).

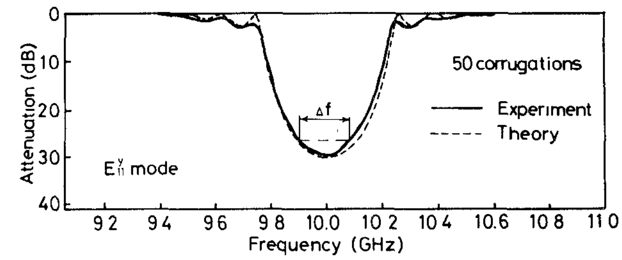

Fig. 11. Design characteristic of the DIG grating and its measured frequency characteristic (h = 12mm, w_1 = 20mm, w_2 = 10.5mm, d = 12mm, and $d_1/d_2 = 1$).

It is worthwhile to discuss here the change in A_{max} when there are some deviations in d_i from the designed values. Fig. 10 is a result of the dependence of A_{max} to d_2/d with the constant d_1. In this case, the center frequency varies slightly. Fig. 10 shows that the ±5-percent deviations in d_2/d from the optimally designed value (0.523) produce a reduction of only 1 percent or less in A_{max}. Considering the above, we have designed a trial grating with $d_1 = d_2 =$ 6 mm, thereby yielding $d_2/d = 0.5$, which has a negligible 4-percent reduction from the optimum value and also shifts the center frequency to $f_0 = 9.97$ GHz.

Fig. 11 shows the attenuation characteristics of the designed trial grating with $N_c = 50$. The solid curve indicates the measured characteristic and the dotted curve indicates the theoretical one calculated from the designed parameters. The measured center frequency, maximum attenuation, and the fractional 3-dB bandwidth all show the excellent agreement with the theory. Also, a surprisingly good agreement between both curves can be found over the whole frequency range of the stopband. However, we also see a slight difference at the frequencies around the first zero of insertion loss appearing on both sides of f_0. The authors currently have no definitive and reasonable way of explaining this difference.

V. CONCLUSIONS

A new and completely theoretical accurate method for the design of dielectric image guide (DIG) gratings has been presented. This method consists of two important stages: one is the stage to calculate the dispersion characteristics of DIG accurately and the other is one to derive the scattering matrix at the junctions of two different sized DIG's completely theoretically. Although the method is approximate since it takes into account only guided surface-wave modes, the effectiveness of the present design procedure has been demonstrated. We are currently studying the design of more practical grating filters using the present method.

ACKNOWLEDGMENT

The authors are deeply indebted to Professor Kei Takiyama of Doshisha University, Kyoto, Japan, for his useful advice and encouragement. The authors also wish to express their thanks to Professor Arthur A. Oliner of Polytechnic Institute of New York, New York, NY, for his useful discussions, advice and constant interest in our work. The cooperation and assistance in both numerical calculations and experiments received from T. Imai is also acknowledged.

REFERENCES

[1] R. M. Knox and P. P. Toulious, "Integrated circuits for millimeter through optical frequency range," in *Proc. Symp. Submillimeter Waves*, MRI (Polytechnic Institute Brooklyn, Brooklyn, New York), Mar. 1970, pp. 497–516.

[2] H. Jacobs and M. M. Chrepta, "Electronic phase shifter for millimeter-wave semiconductor dielectric integrated circuits," *IEEE Trans. Microwave Theory Tech.*, vol. MTT-22, pp. 411–417, Apr. 1974.

[3] T. Itoh, "Inverted strip dielectric waveguide for millimeter-wave integrated circuits," *IEEE Trans. Microwave Theory Tech.*, vol. MTT-24, pp. 821–827, Nov. 1976.

[4] G. L. Matthaei, D. C. Park, Y. M. Kim, and D. L. Johnson, "A study of the filter properties of single and parallel-coupled dielectric-waveguide gratings," *IEEE Trans. Microwave Theory Tech.*, vol. MTT-31, pp. 825–835, Oct. 1983.

[5] D. C. Park, G. L. Matthaei, and M. S. Wei, "Dielectric waveguide grating design for bandstop and bandpass filter applications," in *1984 IEEE/MTTS Intern'l Microwave Symp.*, (San Francisco, CA), May 1984, pap. 7-17.

[6] H. Shigesawa and M Tsuji, "Mode propagation through a step discontinuity in dielectric planar waveguide," *1984 IEEE/MTTS Int. Microwave Symp.*, (San Francisco, CA), May 1984, pap. 5-3.

[7] H. Shigesawa, M. Tsuji, and K. Takiyama, "Dielectric gratings as circuit components in MM and SUBMM -wave regions," in *9th Int. Conf. IR MM Waves*, Takarazuka, Japan, Oct. 1984, pap. T-9-7.

[8] ____, "Microwave network representation of discontinuity in open dielectric waveguides and its applications to periodic structures," in *1985 IEEE/MTTS Int. Microwave Symp.*, (St. Louis, MO), June 1985, pap. Y-2.

[9] ____, "Microwave network approach to dielectric periodic leaky-wave antennae," in *1985 Int. Symp. Antennas Propagat.*, (Kyoto, Japan), Aug. 1985, pap. 022-5.

[10] M. Tsuji, S. Matsumoto, H. Shgigesawa, and K. Takiyama, "Guided-wave experiments with dielectric waveguides having finite periodic corrugation," *IEEE Trans. Microwave Theory Tech.*, vol. MTT-31, pp. 337–344, Apr. 1983.

[11] G. L. Matthaei, "A note concerning modes in dielectric wave guide gratings for filter applications," *IEEE Trans. Microwave Theory Tech.*, vol. MTT-31, pp. 309–312, Mar. 1983.

[12] J. E. Goell, "A circular-harmonic computer analysis of rectangular dielectric waveguides," *Bell Syst. Tech. J.*, vol. 48, pp. 2132–2160, Sept. 1969.

[13] K. Solbach and I. Wolff, "The electromagnetic fields and the phase constants of dielectric image lines," *IEEE Trans. Microwave Theory Tech.*, vol. MTT-26, pp. 266–274, Apr. 1978.

[14] M. Tsuji, S. Suhara, H. Shigesawa, and K. Takiyama, "Submillimeter guided-wave experiments with dielectric rib wave guides," *IEEE Trans. Microwave Theory Tech.*, vol. MTT-29, pp. 547–552, June 1981.

[15] M. J. Shiau, H. Shigesawa, S. T. Peng, and A. A. Oliner, "Mode conversion effects in Bragg reflection from periodic grooves in rectangular dielectric image guide," in *1981 IEEE/MTTS Int. Microwave Symp.*, June 1981, pap. A-5.

Hiroshi Shigesawa (S'62–M'63–SM'85) was born in Hyogo, Japan, on January 5, 1939. He received the B.S., M.S., and Ph.D. degrees in electrical engineering from Doshisha University, Kyoto, Japan, in 1961, 1963, and 1969, respectively.

Since 1963, he has been with Doshisha University. From 1979 to 1980, he was a Visiting Scholar at Microwave Research Institute, Polytechnic Institute of New York, Brooklyn, NY. Currently, he is a professor at the Faculty of Engineering, Doshisha University. His present research activities involve millimeter and submillimeter wave-guiding structures and devices, and scattering problems of electromagnetic wave.

Dr. Shigesawa is a member of the Institute of Electronics and Communication Engineers (IECE) of Japan, the Institute of Electrical Engineers (IEE) of Japan, and Optical Society of America (OSA).

Mikio Tsuji (S'77–M'82) was born in Kyoto, Japan, on September 10, 1953. He received the B.S., M.S., and Ph.D. degrees in electrical engineering from Doshisha University, Kyoto, Japan, in 1976, 1978, and 1985, respectively.

Since 1981, he has been with Doshisha University, where he is now a lecturer. His research activities have been concerned with microwave and submillimeter-wave guiding structures as well as devices of open structures.

Dr. Tsuji is a member of the Institute of Electronics and Communication Engineers (IECE) of Japan.